HHS Public Access

Author manuscript

Antimicrob Agents Chemother. Author manuscript; available in PMC 2026 May 18.

Published in final edited form as:

Antimicrob Agents Chemother. ; : e0184925. doi:10.1128/aac.01849-25.

Strain diversity drives heterogeneous responses to tuberculosis combination therapy

Michelle H. Yoon[1,2], **Peter H. Culviner**[3], **Mariana Pereira Moraes**[1,4], **Hidetomi Nitta**[1], **Nguyen Thuy Thuong Thuong**[5,6], **Sarah M. Fortune**[3], **Bree B. Aldridge**[1,7,8,*]

[1]Department of Molecular Biology and Microbiology, Tufts University School of Medicine, Boston, MA, USA.

[2]Current: Department of Microbial Pathogenesis, Yale School of Medicine, New Haven, CT, USA.

[3]Department of Immunology and Infectious Diseases, Harvard T.H. Chan School of Public Health, Boston, MA, USA.

[4]Current: State University of New York Upstate Medical University, Syracuse, NY, USA.

[5]Oxford University Clinical Research Unit, Ho Chi Minh City, Vietnam.

[6]Centre for Tropical Medicine and Global Health, Nuffield Department of Medicine, University of Oxford, Oxford, UK.

[7]Stuart B. Levy Center for Integrated Management of Antimicrobial Resistance, Tufts University, Boston, MA, USA.

[8]Department of Biomedical Engineering, Tufts University School of Engineering, Medford, MA, USA.

Abstract

Strain diversity in *Mycobacterium tuberculosis* (Mtb) underlies distinct clinical presentations and outcomes, but the range of drug susceptibility phenotypes among clinical isolates is poorly understood. We aimed to identify drug response patterns in phylogenetically diverse clinical isolates to combination treatment. We selected 13 strains out of 641 drug-sensitive clinical isolates that capture local and global phylogenetic diversity and included Erdman ATCC-35801 as a reference. We treated each strain with 10 single drugs, 45 drug pairs, and 20 three-way combinations in standard and cholesterol-rich media. Mtb clinical strains displayed a broad range of drug response phenotypes across the 65 drug combinations and two metabolic conditions tested,

*Corresponding author and lead contact: Bree Aldridge, 136 Harrison Ave, Boston, MA 0211 | bree.aldridge@tufts.edu.

Contributors

MHY, PHC, SMF, and BBA were responsible for conceptualization of the study. MHY and BBA conducted the literature search, developed the figures, and performed formal analysis and writing of the original manuscript. MHY, MPM, and HN were responsible for data curation. MHY, PHC, SMF, and BBA contributed to data interpretation. PHC, NTTT, SMF, and BBA were responsible for funding acquisition and supervision of the study. All authors had access to the study data and contributed to the review and editing of the manuscript.

Declaration of interests

The authors declare no competing interests.

with the most effective drug pairs (based on potency and synergy) varying by strain and metabolic condition. Within our 14-strain panel, strains that were less sensitive to single drugs were also less sensitive to combination treatment, with very few exceptions. For all drug combinations tested, the variation in combination potency was driven primarily by variation among genetically related strains, rather than between strains belonging to disparate lineages. Preclinical regimen design should reflect the diversity of Mtb clinical strains; our data suggest that selecting strains based on the range of drug response phenotypes displayed, rather than by genetic diversity alone, may better account for pathogen diversity. Our findings also show that constituent drug pairs of high-order combinations can be differentially effective against Mtb adapted to different carbon sources. Selection of these pairs should likely involve multiple factors including the infecting strain, metabolic niche, and drug response metrics.

Introduction

Tuberculosis (TB) remains challenging to treat, in part because a subset of patients requires extended treatment. Hard-to-treat disease may have several origins: lesions associated with severe pathologies impede drug penetration and drug susceptibility, and genetic differences among infecting organisms—and the phenotypes they mediate—can manifest in heterogeneous disease presentations and responses to drug treatment.[1–4] Though several studies demonstrate substantial heterogeneity in antibiotic susceptibility, transmission potential, and treatment outcomes among newly emerging *Mycobacterium tuberculosis* (Mtb) clinical strains,[5] bacterial determinants (beyond canonical resistance mutations) associated with unfavorable clinical outcomes have only recently been characterized.[3] Recent studies show that strain-to-strain variation in response to antibiotic and metabolic stress and modest differences in MIC values below clinical breakpoints underlie distinct clinical phenotypes such as treatment failure and cavitary disease.[3,6] However, despite growing evidence that subtle differences in antibiotic susceptibility can lead to divergent clinical outcomes, preclinical drug combination studies focus on a few commonly studied Mtb strains (Erdman, H37Rv, HN878), which may underrepresent the range of drug susceptibility patterns of clinical isolates.[7–10]

Though phenotypic responses to several first- and second-line antibiotics are well characterized across different Mtb phylogenetic lineages,[11–14] TB treatment relies on combination therapy, and clinical outcomes likely reflect strain-dependent differences in drug combination efficacy.[15] Yet, we lack a systematic evaluation and understanding of combination treatment responses across diverse clinical isolates. Here, we provide an analysis of drug responses to 65 unique drug combinations across a phylogenetically diverse panel of Mtb clinical strains in two *in vitro* conditions that model different cell states. Our data allows us to answer several fundamental questions about the impacts of strain variation on combination treatment outcomes: How does the drug susceptibility of clinical isolates vary in response to single drugs and drug combinations? Do genetically related isolates exhibit similar drug susceptibility patterns? Are certain isolates more tolerant to certain combinations, and if so, can we identify any drug-dependent or strain-dependent patterns? Finally, can we reasonably predict how susceptible a given isolate is to combination treatment based on its susceptibility to single drugs - that is, can we screen problematic

isolates based on single drug susceptibility? The variation we highlight across strains and drug combination treatments, in different metabolic conditions, may aid future combination treatment optimization in accounting for pathogen diversity, with implications for de-risking, revamping, and accelerating drug regimen design.

Results

Clinical isolates were obtained from TB patients with diverse clinical presentations including lung cavitation and treatment failure, as detailed in Stanley et al., 2024.[3] We selected 13 strains that capture local and global phylogenetic diversity, including two strains from subclades of L1.2 (185 and 355), two strains from the locally expanded L1.1.1.1 (139 and 358), two outgroup strains in L1.1.1.1 (414 and 617), a strain each from the L4.1 Erdman clade and L4.4 H37Rv clade (082 and 084, respectively), a strain from the proto-Beijing L2.1 (245) and four strains from the expanded L2.2 lineage (044, 070, 478, 545) (Figure 1A). We selected ten antibiotics that represent a broad range of mechanisms of action (Supplementary Table 1) and included Erdman ATCC 35801, commonly used in systematic drug combination studies,[7,8] as a reference. Based on the phylogenetic tree of the 14 strains, we found that the strains bifurcated into two major groups: Lineage 1 (Figure 1A, orange) and Lineages 2 and 4 (Figure 1A, blue). We manually classified the strains into these two groups for ease of interpretation.

Mtb occupies metabolically distinct niches *in vivo*.[2] Cholesterol is a key carbon source in lipid-rich environments within granulomas,[16,17] and studies demonstrate substantial heterogeneity in drug response between Mtb acclimated to different carbon sources.[2,18,19] Both glycerol- (called standard here) and lipid-based *in vitro* models (including cholesterol) have been validated as predictive of treatment outcomes *in vivo*.[7,8] To account for condition-dependent variation in drug response phenotypes, we conducted all drug combination assays in standard conditions and in a medium with cholesterol as the sole carbon source (called cholesterol here). We note that a subset of strains—245, 358, and 478—arrested growth in cholesterol and were excluded from analysis in this condition.

We observed substantial variation in doubling times across clinical isolates in both standard (14 to 21 hours) and cholesterol (51 to 104 hours) conditions. To compare drug and drug combination efficacy across different strains and conditions, we used GR metrics, which normalize drug treatment response to the untreated growth rate of each strain. Specifically, we used GR_{max}, the maximum growth rate inhibition, to compare drug and drug combination responses across 14 Mtb strains and two *in vitro* conditions. We also computed commonly used drug response metrics such as inhibitory concentrations (ICs) and drug interaction scores (fractional inhibitory concentrations, FICs, Figure 1B, top). A subset of drugs failed to achieve at least 90% growth inhibition in several strains; we therefore used IC_{50} values to interpret phenotypic responses to single drugs and to compute drug interaction scores at the IC_{50} (FIC_{50}). Negative, zero, and positive $\log_2 FIC_{50}$ values denote synergy, additivity, and antagonism, respectively.

To characterize drug response patterns across our panel of 14 Mtb strains, we treated each strain with ten antibiotics in standard and cholesterol conditions. For each drug treatment,

we generated dose response curves from which we calculated GR_{max} and IC_{50} values, resulting in 280 metrics in standard and 220 metrics in cholesterol. In both conditions, we observed strain-to-strain differences in GR_{max} for all ten drugs tested (Figure 1C). For select drugs such as bedaquiline, pretomanid, and moxifloxacin in standard, and bedaquiline, pretomanid, and TBA-3731 in cholesterol, IC_{50} values varied by nearly 10-fold between strains (Figure 1D). We observed that most clinical isolates are more drug tolerant than Erdman in both standard and cholesterol (Supplementary Figure 1). Notably, bedaquiline and pretomanid displayed the greatest variability in IC_{50} values across all strains in both conditions (Figure 1D), suggesting that despite their use in new regimens, their efficacy may be inconsistent across clinical strains.

We next asked whether treating Mtb with drug pairs improves treatment efficacy relative to single drugs, based on changes in GR_{max} values. To quantify GR_{max} improvement, we calculated the difference between the GR_{max} of a drug pair and the GR_{max} of its constituent singles, with negative values indicating improvement. Across all strains in standard medium, the addition of bedaquiline or pretomanid to another drug improved the GR_{max} of the other drug, with improvement observed in 216/224 (96.5%) drug pairs containing either bedaquiline or pretomanid (Figure 2A, left; Supplementary Figure 3, top). Given that bedaquiline and pretomanid are the two most potent single drugs in standard medium, we hypothesized that combining any drug with another drug that is less potent than itself will invariably improve the GR_{max} of the less potent drug. We found that this was generally the case, but not to the same extent as bedaquiline or pretomanid. For instance, SQ109, linezolid, and isoniazid also improved the GR_{max} of drugs less potent than itself in a majority of drug pairs (84/98 drug pairs or 85.7%, 69/84 drug pairs or 82.1%, 67/70 or 95.7%, respectively), but they improved the GR_{max} of more potent drugs (such as bedaquiline and pretomanid) in only a subset of strains (Supplementary Figure 2, top). However, we did not observe this pattern in other drugs such as moxifloxacin or rifampicin—in these drugs, GR_{max} improvement was less predictable (Supplementary Figure 2, top). These findings suggest that (i) in some cases, GR_{max} improvement of drug pairs can be predicted based on the potency of the individual drugs being combined and (ii) bedaquiline and pretomanid may have intrinsic properties that allow them to optimize drug combination efficacy in diverse strain backgrounds beyond what would be expected based on potency alone. In cholesterol, however, neither BDQ nor PRE improved GR_{max} across all combinations and strains (Figure 2A, right; Supplementary Figure 2, bottom; Supplementary Figure 3). Instead, the magnitude of GR_{max} improvement for drug pairs containing BDQ or PRE varied by strain, suggesting that combination efficacy in cholesterol depends more on strain-specific susceptibility patterns to drug pairs than by the intrinsic properties of individual drugs.

The drug susceptibility profile of a specific Mtb strain is typically defined based on its minimum inhibitory concentration (MIC) values to select single drugs, even though TB patients are treated with drug combinations. We therefore asked whether drug response phenotypes to single drugs provide any predictive insight into strain-specific phenotypic responses to combination treatment. We compared GR_{max} values across three different treatment modalities—single drugs (10 drugs), drug pairs (45 pairs), and three-way combinations (20 combinations)—for each strain (Figure 2B; Supplementary Figure 4;

Supplementary Table 2; Supplementary Table 3). This comparison addressed two related questions: (1) within our 14-strain subset, are strains that are more difficult to treat with single drugs also more difficult to treat with drug combinations, and (2) between different treatment modalities, does GR_{max} change in a strain-dependent manner, or does it follow a generalizable trend? In both standard and cholesterol, we found that strains that are less sensitive to single drugs are also less sensitive to drug pairs and three-way combinations on average (Figure 2B; Supplementary Figure 4), as these strains (represented in red) occupy the upper range in GR_{max} across nearly all drugs in the three treatment modalities tested (Figure 2B; Supplementary Figure 4). We conclude that the stratification of strains by single-drug susceptibility is largely preserved between treatment modalities. An exception was isolate 355 in standard medium; although more tolerant to single drugs than most other strains, its GR_{max} was greatly improved by treatment with drug pairs, especially those containing SQ109, moxifloxacin, rifampin, and TBA-3731 (Figure 2B, left).

We then evaluated whether three-way combinations provide further improvement in treatment efficacy over drug pairs. Due to experimental constraints, we restricted the three-way panel to six drugs with major clinical relevance to contemporary TB treatment and regimen design (BDQ, PRE, LIN, INH, MOX, and RIF).[20–23] Given that only six drugs were tested in three-way combinations, as opposed to ten drugs in drug pairs, comparisons were limited to shared compounds. In both standard and cholesterol, there was no improvement in GR_{max} in three-way combinations over drug pairs, suggesting that high-order combinations do not provide additional improvement over drug pairs in the conditions tested (Supplementary Figure 4).

To improve the resolution of strain-specific phenotypic responses to drug combination treatment, we decomposed averaged drug combination data into all individual drug pairs (Figure 3A) and three-way combinations (Figure 3B) tested. This allowed us to ask several questions: (1) are hard-to-treat strains (defined by low susceptibility to single drugs) more tolerant to all drug combinations, or do specific combinations sensitize them, and (2) do some drug combinations display larger variability in GR_{max} than others, and if so, do certain strains drive this variability? We found that in both standard and cholesterol conditions, hard-to-treat strains are more tolerant to nearly all drug pairs and three-way combinations tested (Figure 3A and 3B, violin plots), suggesting that strains that are tolerant to single drugs are expected to be more difficult to treat with drug combinations. Regardless, a small subset of drug combinations was effective against select hard-to-treat strains. For example, of all 45 drug pairs and 20 three-way combinations tested, pretomanid+rifampin (PRE+RIF), pretomanid+telacebec (PRE+Q203), and isoniazid+pretomanid+rifampin (INH+PRE+RIF) were the only drug combinations that induced a cytotoxic effect in isolate 139 in standard (Figure 3A and 3B, violin plots for standard). Similarly, bedaquiline+isoniazid (BDQ+INH) and bedaquiline+TBA-3731 (BDQ+TBA) also showed increased potency against isolate 185 (Figure 3A, violin plot for standard). These examples highlight the potential of targeted combinations to sensitize strains that may otherwise be tolerant to a broad swath of treatment options.

Across all drug pairs and three-way combinations, we sought to identify a quantitative relationship between drug combination potency, as determined by GR_{max}, and the

magnitude of strain-to-strain variability, as determined by the coefficient of variation (CV) (Figure 3A and 3B, gray bar plots). There was no correlation between combination potency and the magnitude of strain-to-strain variability, but a small subset of potent drug combinations—bedaquiline+rifampin (BDQ+RIF), bedaquiline+pyrazinamide (BDQ+PZA), and bedaquiline+isoniazid+moxifloxacin (BDQ_INH+MOX) in standard medium—were more variable than others in the same condition (Figure 3A and 3B, gray bar plots for standard). Notably, we found that strain-to-strain variability in GR_{max} to single drugs (Supplementary Figure 5) is not correlated with variability in GR_{max} to drug pairs (Figure 3A, gray bar plots for standard). That is, although bedaquiline and pretomanid exhibit the most strain-to-strain variability in GR_{max} (Supplementary Figure 5), combining pretomanid with another drug tended to reduce the amount of variability; in contrast, pairing bedaquiline with another drug tended to increase variability (Figure 2B, left). Moreover, we found that three-way combinations do not reduce variability relative to drug pairs (Figure 3A and 3B, gray bar plots; Supplementary Figure 6), suggesting that increasing the number of drugs does not mitigate strain-to-strain differences in single drug response.

We next asked whether specific strains or strain groups drive the variation in GR_{max} observed in each of the drug combinations tested. We partitioned the total variance in GR_{max} for each drug combination into three components: variance within lineage 1 strains, variance within strains in lineages 2 and 4, and variance between the two strain groups (Figure 3A and 3B, stacked bar plots). Strikingly, for all combinations tested, the total variance was driven primarily by variability in GR_{max} within strain groups, rather than between (Figure 3A and 3B, stacked bar plots), suggesting that genetically related strains do not necessarily exhibit similar drug response phenotypes.

Though we demonstrate that three-way combinations do not improve drug potency over drug pairs in any one condition, TB treatment still necessitates high-order combinations since its constituent drug pairs may target different metabolic and physical niches. We sought to identify candidate drug pairs, based on their GR_{max} and FIC_{50} values, that could potentially be effective across diverse strain backgrounds and different *in vitro* conditions. A few drug pairs were both potent and synergistic in standard and cholesterol (Figure 4A, orange), but only a small subset of these pairs—pretomanid+rifampin (PRE+RIF) and rifampin+SQ109 (RIF+SQ109)—were shared between the two conditions (Figure 4A, orange). For all drug pairs, the standard deviation in potency (horizontal error bars) and synergy (vertical error bars) varied greatly, suggesting that drug pairs that satisfy both criteria (potent and synergistic) vary by individual strain. We further demonstrate limited correlation between potency and synergy, as drug pairs that are potent in both conditions (Figure 4B, left) and synergistic in both conditions (Figure 4B, right) vary. Altogether, these data further support our understanding that different drug pairs target metabolically heterogeneous Mtb, and the selection of these pairs relies on a multitude of factors including genetic background, metabolic state, and a consideration of several drug response metrics.

Discussion

Altogether, we demonstrate substantial heterogeneity in drug response to combination treatment across our 14-strain panel, with certain strains exhibiting attenuated sensitivity

to nearly all drugs and drug combinations tested. Importantly, many clinical isolates were less sensitive to combination treatment than commonly studied strains such as Erdman, and treatment efficacy of drug combinations varied greatly by strain, especially those that included drugs that are relevant in the clinic and in preclinical studies. Our findings highlight the importance of studying the effects of drug combination treatments in phenotypically diverse Mtb strains, particularly to define the upper bounds of drug tolerance.

While identifying genetic resistance markers remains essential in understanding the causes of severe disease pathologies and treatment failure, an increasing body of work shows that physiological adaptations such as altered respiration and energy metabolism, metabolic reprogramming, and upregulation of multidrug efflux pumps can broadly reduce drug susceptibility independent of genotype.[24–27] Our results support the understanding that such mechanisms, not readily identified via genomic analyses alone, may underlie broad-spectrum drug tolerance to a larger extent than expected: strains that are less susceptible to single agents often remain recalcitrant to high-order drug combinations, even when those combinations include drugs with distinct mechanisms of action. That is, increasing the number of drugs in a combination failed to mitigate relative drug tolerance, or reduce the magnitude of strain-to-strain variability in drug response. These findings suggest that high-order combinations alone are insufficient to rescue certain forms of intrinsic or acquired drug tolerance.

Strikingly, strain-to-strain variation in drug response was driven primarily by the susceptibility profiles of individual strains, rather than by lineage identity. Strain phenotypes are likely driven by mutations arising on terminal branches, or other contemporaneous changes that are heritable yet appear randomly distributed across the phylogenetic space due to our limited resolution (n = 14 strains). Additionally, adaptations shaped by various facets of the host environment that modulate drug response may have been selected for during infection and retained *in vitro*. Our results also have implications in designing strain panels for preclinical combination design studies; we propose that selecting strains based on phenotypic, in addition to genetic, diversity may more effectively capture strain diversity. Overall, our findings advocate for a holistic approach to studying the effects of combination therapy—one that probes both the upper and lower bounds of drug susceptibility across phenotypically diverse strains and contextualizes these phenotypes in several host-relevant metabolic conditions.

There are several limitations to our study. First, although our 14-strain panel spans both local and global phylogenetic diversity, it is derived from a single geographic cohort and thus represents a limited fraction of the global Mtb population. Further expanding the strain panel in scope and size may provide new insight into drug response traits underlying heterogeneous treatment outcomes. Second, though our cholesterol model reflects host-relevant carbon sources, it does not fully recapitulate the lesion microenvironment such as immune pressure, hypoxic stress, and nutrient restriction. Additionally, the cholesterol condition alone only represents a fraction of the metabolic diversity of Mtb during host infection. Future combination studies should include multiple host-like *in vitro* conditions to account for this diversity. Finally, a subset of strains arrested growth in cholesterol medium

and were thus excluded from further analysis in that condition, limiting direct comparisons across the complete strain panel.

The current first-line regimen and several other drug combinations used in the clinic vary in treatment efficacy among TB patients.[28,29] To mitigate this variability, it is crucial for key processes in drug combination design and optimization to account for strain-to-strain differences in drug susceptibility. Our study demonstrates that strain variation in drug combination responses may explain some of the differences in drug responses observed in the clinic, which suggests that introducing strain diversity into these preclinical studies has major implications in optimizing and derisking drug regimen design.

Methods

Antimicrobials, dispensing, and drug combination design

A complete list of antibiotics used in this study is provided in Supplementary Table 1. 50% inhibitory concentrations (IC_{50}) were calculated for all antibiotics in two different *in vitro* models with different carbon sources: standard (sugar-rich) and cholesterol (lipid-rich). Acclimation procedures are detailed in the Supplementary Material. For drug combinations, equipotent mixtures of antibiotics were created by aligning the IC_{50} value of each constituent drug to the same dose level.[30] Initial IC_{50} measurements were made using 14 doses with 2-fold spacing, whereas subsequent experiments used a 1.5-fold dose resolution across 10 doses.

Strains and culturing

All strains used in this study were prepared and cultured in a 7H9 broth supplemented with 0.05% Tween 80, 0.2% glycerol, and 10% Middlebrook OADC (referred to as standard medium in the main text) and stored in −80°C until use. Frozen 1ml stocks of Mtb were added to 9ml of standard medium and grown in a 37°C shaking incubator to mid-log phase (optical density at 600nm, or OD_{600}, between 0.4 and 0.8).

Drug treatment assays

Dose response assays for drug combinations were designed using the DiaMOND (diagonal measurement of *n*-way drug interactions) method, which optimizes traditional checkerboard assays to measure equipotent mixtures of drugs.[31] This allows efficient measurements of drug interactions in a large number of drug combinations that would otherwise be impractical with traditional methods.

50μl of Mtb grown in either standard or cholesterol medium was back-diluted to an OD_{600} of 0.05, added to drug-treated 384-well plates, and incubated at 37°C in humidified bags to prevent evaporation. Edge wells (top and bottom rows, left- and right-most columns) contained only media and were excluded from analysis. OD_{600} was measured at two time points for each strain using a Synergy Neo2 Hybrid Multi-Mode Reader. For both standard and cholesterol conditions, OD_{600} was measured immediately following inoculation (day 0) and at the terminal time point, which corresponds to 5 days post-inoculation (Day 5) for standard and 12 days post-inoculation (day 12) for cholesterol. The difference in incubation

time between these two conditions reflect the slower growth kinetics of Mtb in cholesterol medium. These time points were identified as being predictive of treatment outcomes *in vivo* and were selected in prior DiaMOND-based studies to allow consistent drug exposure time relative to condition-dependent doubling times.[8]

Data processing and DiaMOND metric calculation

OD_{600} data were processed using custom MATLAB analysis scripts. Raw data were first derandomized and then background-subtracted using the median OD_{600} value of the media-only edge wells. Drug-treated wells were then normalized to the mean OD_{600} value of the untreated controls on the same plate. To generate dose response curves ranging from 0 (no growth inhibition) to 1 (complete growth inhibition), normalized OD_{600} values were subtracted from 1. Each resulting dose-response curve (single drug or drug combination) was fit to a three-parameter Hill function, and the resulting Hill curve parameters were used to calculate inhibitory concentrations (ICs). Calculation of growth rate inhibition (GR) and drug interaction metrics are detailed in the Supplementary Material.

Phylogenetic tree construction

A core genome phylogenetic tree was constructed by downloading complete genomes for the relevant bacterial strains from NCBI. The Erdman ATCC 35801 strain was used as the reference genome. Paired-end FASTQ files for each strain were aligned to the reference genome, and variants were identified for each strain using the ‘bcftools’ package in Python. Core genome alignments were generated, and evolutionary relationships between each strain and the reference genome were summarized using ‘parsnp’ and ‘harvesttools’ packages. A maximum-likelihood phylogenetic tree was then constructed using the ‘IQ-TREE’ package, which evaluates multiple nucleotide substitution models and selects the best-fitting model. Scripts were written in Python 3 and Bash, and the final phylogenetic tree (Figure 1A) was visualized using the ‘tree’ package in R.

Statistics and data reproducibility

All experiments included in this study were performed in three biological replicates excluding single drug dose response experiments in standard (Figure 1), where six biological replicates were used instead. Single-drug dose-response curves in standard medium were measured in two independent experiments (n = 3 biological replicates each) and pooled to improve the precision and reproducibility of fitted single drug metrics.[32,33] For each strain and drug treatment, the median $\log_{10}IC_{50}$ (for single drugs), $\log_2FIC_{50}$ (for drug combinations), and GR_{max} (for drug combinations) value across three biological replicates (for drug combinations and single drugs in cholesterol) and six biological replicates (for single drugs in standard) were measured and represented in the figures.

Supplementary Material

Refer to Web version on PubMed Central for supplementary material.

Acknowledgements

This study was funded by the National Institute of Health (P01AI143575 [SMF], 1F32AI174653 [PHC], UM1AI179699 [BBA]), the Wellcome Intermediate Fellowship (2026724/Z/17/Z [NTTT]), and the Gates Foundation (INV-027276 [BBA]). The conclusions and opinions expressed in this work are those of the author(s) alone and shall not be attributed to the Gates Foundation. Under the grant conditions of the Foundation, a Creative Commons Attribution 4.0 License has already been assigned to the Author Accepted Manuscript version that might arise from this submission. Please note works submitted as a preprint have not undergone a peer review process.

Role of the funding source

The funders of the study had no role in study design, data collection, data analysis, data interpretation, or writing of the manuscript.

Data availability

Whole-genome sequences of all strains used in this study are available through the National Center for Biotechnology Information Sequence Read Archive (SRA) under the accession number PRJNA950969. Accession numbers of individual strains are listed in the Supplementary Material (Supplementary Table 4). All equations used to quantify drug response in this study are listed in the Methods section and the Supplementary Material (Supplementary Methods). The *in vitro* data used in this study and the scripts required to generate the figures are available on Figshare.[34–36]

References

1. Strydom N et al. Tuberculosis drugs' distribution and emergence of resistance in patient's lung lesions: A mechanistic model and tool for regimen and dose optimization. PLOS Medicine 16, e1002773 (2019).
2. Lenaerts A, Barry CE & Dartois V Heterogeneity in tuberculosis pathology, microenvironments and therapeutic responses. https://doi.org/10.1111/imr.12252 doi:10.1111/imr.12252.
3. Stanley S et al. Identification of bacterial determinants of tuberculosis infection and treatment outcomes: a phenogenomic analysis of clinical strains. The Lancet Microbe 5, e570–e580 (2024). [PubMed: 38734030]
4. Shamputa IC et al. Genotypic and Phenotypic Heterogeneity among Mycobacterium tuberculosis Isolates from Pulmonary Tuberculosis Patients. Journal of Clinical Microbiology https://doi.org/10.1128/jcm.42.12.5528-5536.2004 (2004) doi:10.1128/jcm.42.12.5528-5536.2004.
5. Peters JS et al. Genetic Diversity in Mycobacterium tuberculosis Clinical Isolates and Resulting Outcomes of Tuberculosis Infection and Disease. Annual Review of Genetics 54, 511–537 (2020).
6. Colangeli R et al. Bacterial Factors That Predict Relapse after Tuberculosis Therapy. N Engl J Med 379, 823–833 (2018). [PubMed: 30157391]
7. Larkins-Ford J, Degefu YN, Van N, Sokolov A & Aldridge BB Design principles to assemble drug combinations for effective tuberculosis therapy using interpretable pairwise drug response measurements. Cell Reports Medicine 3, 100737 (2022).
8. Larkins-Ford J et al. Systematic measurement of combination-drug landscapes to predict in vivo treatment outcomes for tuberculosis. cels 12, 1046–1063.e7 (2021).
9. Omollo C et al. Developing Synergistic Drug Combinations To Restore Antibiotic Sensitivity in Drug-Resistant Mycobacterium tuberculosis. Antimicrobial Agents and Chemotherapy https://doi.org/10.1128/aac.02554-20 (2021) doi:10.1128/aac.02554-20.
10. Sarathy JP et al. A Novel Tool to Identify Bactericidal Compounds against Vulnerable Targets in Drug-Tolerant M. tuberculosis found in Caseum. mBio https://doi.org/10.1128/mbio.00598-23 (2023) doi:10.1128/mbio.00598-23.

11. The CRyPTIC Consortium and the 100, 000 Genomes Project. Prediction of Susceptibility to First-Line Tuberculosis Drugs by DNA Sequencing. New England Journal of Medicine https://doi.org/10.1056/NEJMoa1800474 (2018) doi:10.1056/NEJMoa1800474.
12. Rashid F, Iqbal S, Tahseen S & Zhao Y Investigation of bedaquiline heteroresistance among Mycobacterium tuberculosis isolates from Pakistan. Microbiology Spectrum https://doi.org/10.1128/spectrum.02181-24 (2025) doi:10.1128/spectrum.02181-24.
13. Farhat MR et al. Rifampicin and rifabutin resistance in 1003 Mycobacterium tuberculosis clinical isolates. J Antimicrob Chemother 74, 1477–1483 (2019). [PubMed: 30793747]
14. Variability in intrinsic drug tolerance in Mycobacterium tuberculosis corresponds with phylogenetic lineage | Antimicrobial Agents and Chemotherapy. https://journals.asm.org/doi/10.1128/aac.00996-25#SuF2.
15. Connolly LE, Edelstein PH & Ramakrishnan L Why Is Long-Term Therapy Required to Cure Tuberculosis? PLOS Medicine 4, e120 (2007). [PubMed: 17388672]
16. Soto-Ramirez MD et al. Cholesterol plays a larger role during *Mycobacterium tuberculosis in vitro* dormancy and reactivation than previously suspected. Tuberculosis 103, 1–9 (2017). [PubMed: 28237027]
17. Pawełczyk J et al. Cholesterol-dependent transcriptome remodeling reveals new insight into the contribution of cholesterol to Mycobacterium tuberculosis pathogenesis. Sci Rep 11, 12396 (2021). [PubMed: 34117327]
18. Cooper SK et al. Heterogeneity in immune cell composition is associated with Mycobacterium tuberculosis replication at the granuloma level. Front. Immunol 15, (2024).
19. Dhar N, McKinney J & Manina G Phenotypic Heterogeneity in Mycobacterium tuberculosis. Microbiology Spectrum https://doi.org/10.1128/microbiolspec.tbtb2-0021-2016 (2016) doi:10.1128/microbiolspec.tbtb2-0021-2016.
20. Rifapentine and isoniazid once a week versus rifampicin and isoniazid twice a week for treatment of drug-susceptible pulmonary tuberculosis in HIV-negative patients: a randomised clinical trial. The Lancet 360, 528–534 (2002).
21. Conradie F et al. Treatment of Highly Drug-Resistant Pulmonary Tuberculosis. New England Journal of Medicine 382, 893–902 (2020). [PubMed: 32130813]
22. Nyang'wa B-T et al. A 24-Week, All-Oral Regimen for Rifampin-Resistant Tuberculosis. New England Journal of Medicine 387, 2331–2343 (2022). [PubMed: 36546625]
23. Gillespie SH et al. Four-Month Moxifloxacin-Based Regimens for Drug-Sensitive Tuberculosis. New England Journal of Medicine 371, 1577–1587 (2014). [PubMed: 25196020]
24. Vilchèze C et al. Enhanced respiration prevents drug tolerance and drug resistance in *Mycobacterium tuberculosis*. Proceedings of the National Academy of Sciences 114, 4495–4500 (2017).
25. Schami A et al. Drug resistant Mycobacterium tuberculosis strains have altered cell envelope hydrophobicity that influences infection outcomes in human macrophages. Sci Rep 14, 30840 (2024). [PubMed: 39730579]
26. Singha B et al. Metabolic Rewiring of Mycobacterium tuberculosis upon Drug Treatment and Antibiotics Resistance. Metabolites 14, 63 (2024). [PubMed: 38248866]
27. Balganesh M et al. Efflux Pumps of Mycobacterium tuberculosis Play a Significant Role in Antituberculosis Activity of Potential Drug Candidates. Antimicrobial Agents and Chemotherapy https://doi.org/10.1128/aac.06003-11 (2012) doi:10.1128/aac.06003-11.
28. Trauer JM et al. The Importance of Heterogeneity to the Epidemiology of Tuberculosis. 10.1093/cid/ciy938.
29. Faustini A, Hall AJ & Perucci CA Tuberculosis treatment outcomes in Europe: a systematic review. European Respiratory Journal 26, 503–510 (2005). [PubMed: 16135735]
30. Cokol M, Kuru N, Bicak E, Larkins-Ford J & Aldridge BB Efficient measurement and factorization of high-order drug interactions in Mycobacterium tuberculosis. Science Advances https://doi.org/10.1126/sciadv.1701881 (2017) doi:10.1126/sciadv.1701881.
31. Van N, Degefu YN & Aldridge BB Efficient Measurement of Drug Interactions with DiaMONDDiagonal measurement of n-way drug interactions (DiaMOND)(Diagonal Measurement of N-Way Drug InteractionsDiagonal measurement of n-way drug interactions

(DiaMOND)). in Mycobacteria Protocols (eds. Parish T & Kumar A) 703–713 (Springer US, New York, NY, 2021). doi:10.1007/978-1-0716-1460-0_30.

32. Altman N & Krzywinski M Sources of variation. Nature Methods 12, 5–6 (2015).
33. Blainey P, Krzywinski M & Altman N Replication. Nature Methods 11, 879–880 (2014). [PubMed: 25317452]
34. Yoon M Raw data for pairwise and three-way drug combinations pertaining to all figures. 1031058 Bytes figshare 10.6084/M9.FIGSHARE.30280441 (2025).
35. Yoon M Raw data for single drug treatments pertaining to figures 1 and 2. 67785 Bytes figshare 10.6084/M9.FIGSHARE.30280447 (2025).
36. Yoon M Scripts for generating all figures. 116841 Bytes figshare 10.6084/M9.FIGSHARE.30280462 (2025).

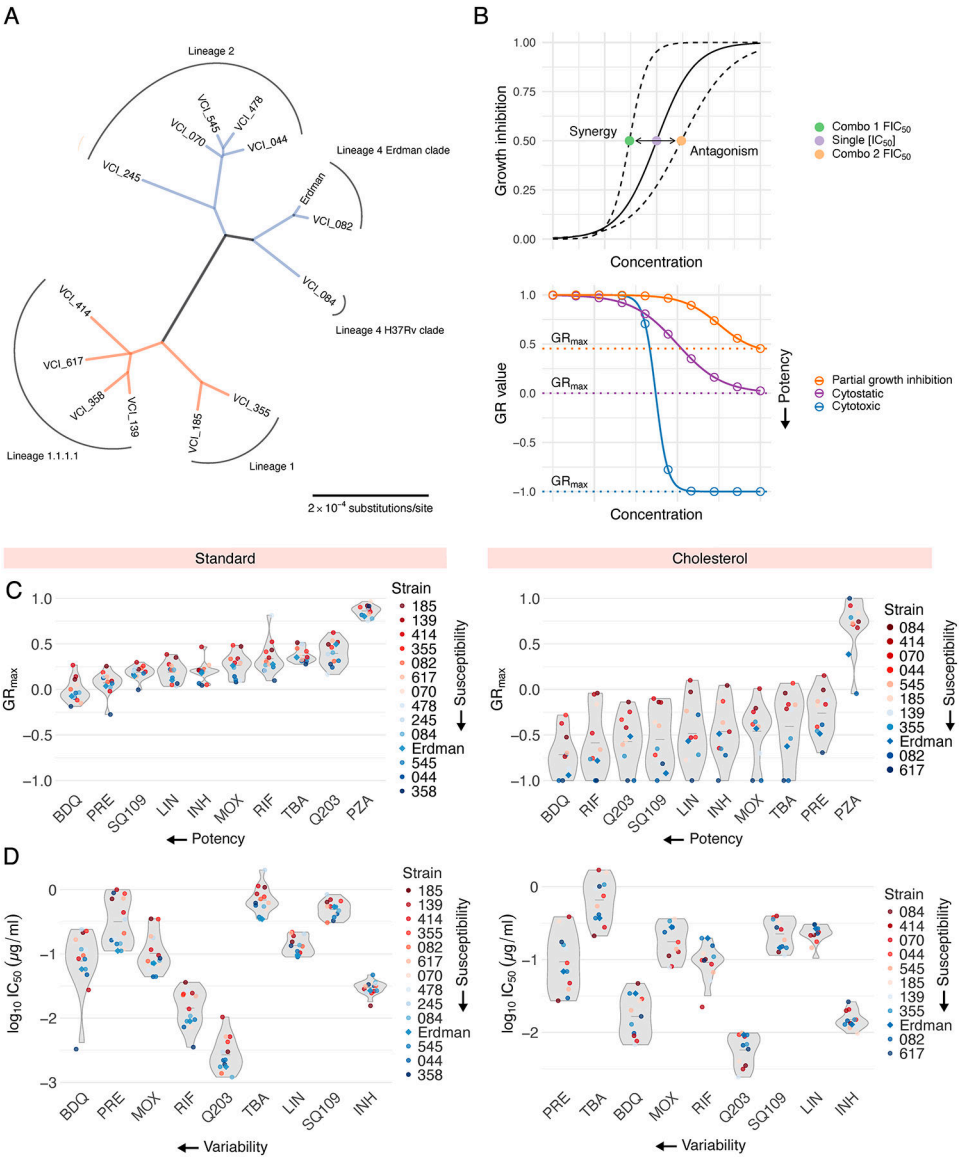

Figure 1. Susceptibility profiles of phylogenetically diverse Mtb clinical isolates to ten antibiotics.

(A) Unrooted maximum-likelihood phylogenetic tree of the 14 Mtb strains studied in this work, as determined by core gene alignments. Scale bar represents substitutions per nucleotide. Colors indicate strain groups defined for the interpretation of this work. (B) Schematics of drug interaction (top) and potency (bottom) metrics computed via DiaMOND. (Top) The solid-line dose response curve represents the inhibitory effect of a single drug. Shifts in the left and right directions indicate synergy and antagonism, respectively, when combined with another drug. (Bottom) Dose response curves indicate a cytotoxic response (blue), cytostatic response (purple), and partial growth inhibition (orange). (C) GR_{max} values of ten antibiotic treatments across 14 strains in standard (left) and 11 strains in cholesterol (right). Strains are colored from least drug-susceptible (red), to most drug-susceptible (blue) (Supplementary Figure 1). Antibiotics are ordered from most potent to least potent, from left to right, respectively. Each point represents the median GR_{max} value across six biological

replicates in standard and three biological replicates in cholesterol. (D) Half-maximal inhibitory concentrations (IC50) of nine antibiotic treatments across 14 strains in standard (left) and 11 strains in cholesterol (right). PZA is excluded due to inactivity as a single agent. Strains are colored from least drug-susceptible (red) to most drug-susceptible (blue). Antibiotics are ordered from most variable (highest coefficient of variation, CV) to least variable (lowest CV), from left to right, respectively. Each point represents the median log10IC50 value across six biological replicates in standard and three biological replicates in cholesterol.

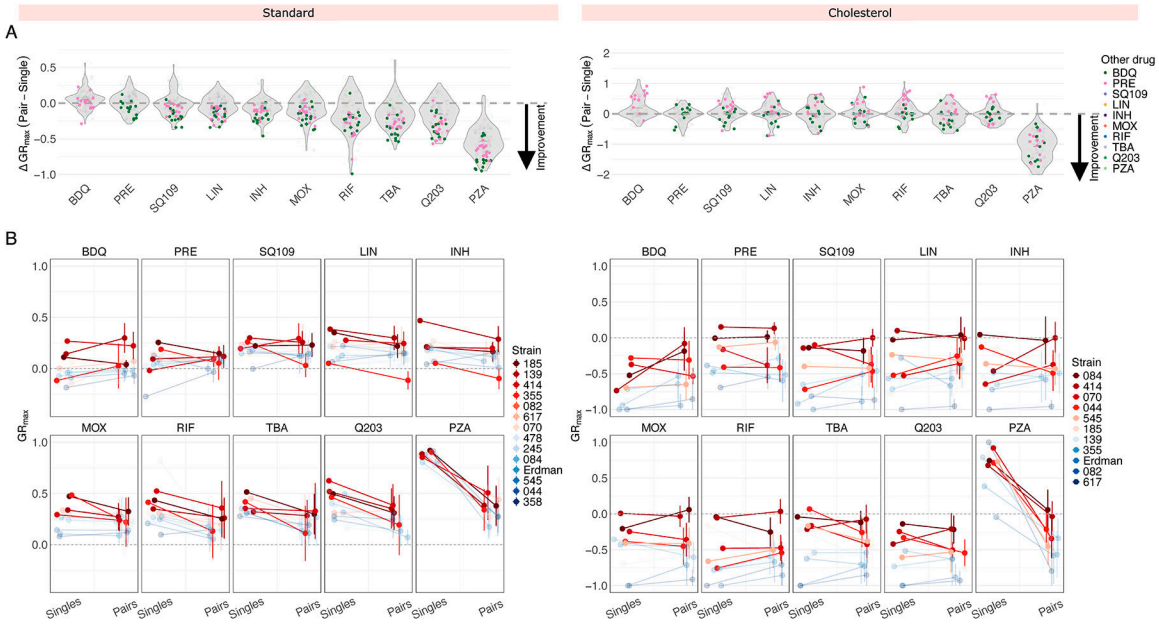

Figure 2. Comparison of GR_{max} values between different drug modalities.

(A) Change in GR_{max} between single drug and pairwise treatments in standard (left) and cholesterol (right) conditions. Each point denotes a ΔGR_{max} value of a drug pair for an individual isolate and represents the median GR_{max} value across three biological replicates. Drug pairs containing bedaquiline and pretomanid are highlighted in green and pink, respectively. A ΔGR_{max} value less than zero indicates an improvement in GR_{max} when a single drug is combined with a second drug (e.g., when BDQ is combined with LIN, or when INH is combined with MOX). (B) Comparison of GR_{max} values between single drugs and their nine corresponding drug pairs (Supplementary Table 2) in standard (left) and cholesterol (right) conditions. Each panel represents a single drug on the left side and the mean GR_{max} value of its nine corresponding drug pairs on the right side. Vertical bars represent the standard deviation of the mean GR_{max} value. Each point represents the median GR_{max} value across three biological replicates and corresponds to an individual strain. The four least susceptible strains for each condition are highlighted in red. (Note: opacity adjustments are not reflected in the legend.)

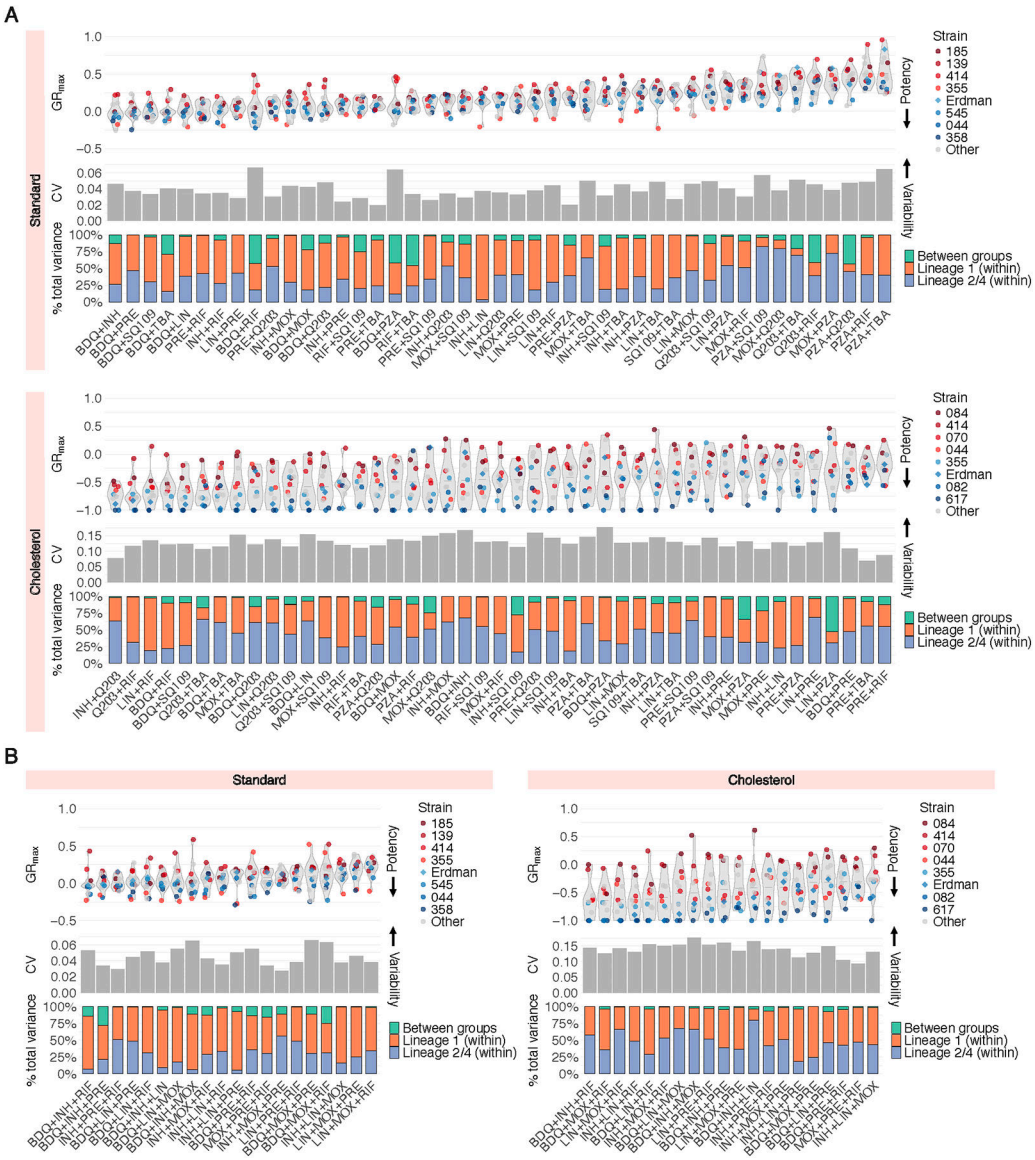

Figure 3. Susceptibility profiles of Mtb clinical isolates to drug pairs and high-order combinations.

Drug potency and strain variability metrics of (A) 45 drug pairs and (B) 20 three-way combinations tested in standard and cholesterol. For each condition: (top) violin plots represent the GR_{max} range across all clinical strains tested. The four least drug-susceptible strains and the four most drug-susceptible strains (Fig. 1D) are highlighted in red and blue, respectively. All other strains are represented in grey. Each point represents the median GR_{max} value across three biological replicates. (Middle) Each bar represents the coefficient of variation (CV) of GR_{max} values across 14 strains in standard and 11 strains in cholesterol for each drug pair. (Bottom) Each stacked bar represents the variance decomposition of the GR_{max} values across 14 strains in standard and 11 strains in cholesterol for each drug pair. The green bar represents the percent total variance attributable to variance between lineage 1 and lineages 2 and 4; the orange bar represents the percent total variance attributable to

variance within lineage 1; the blue bar represents the percent total variance attributable to variance within lineages 2 and 4.

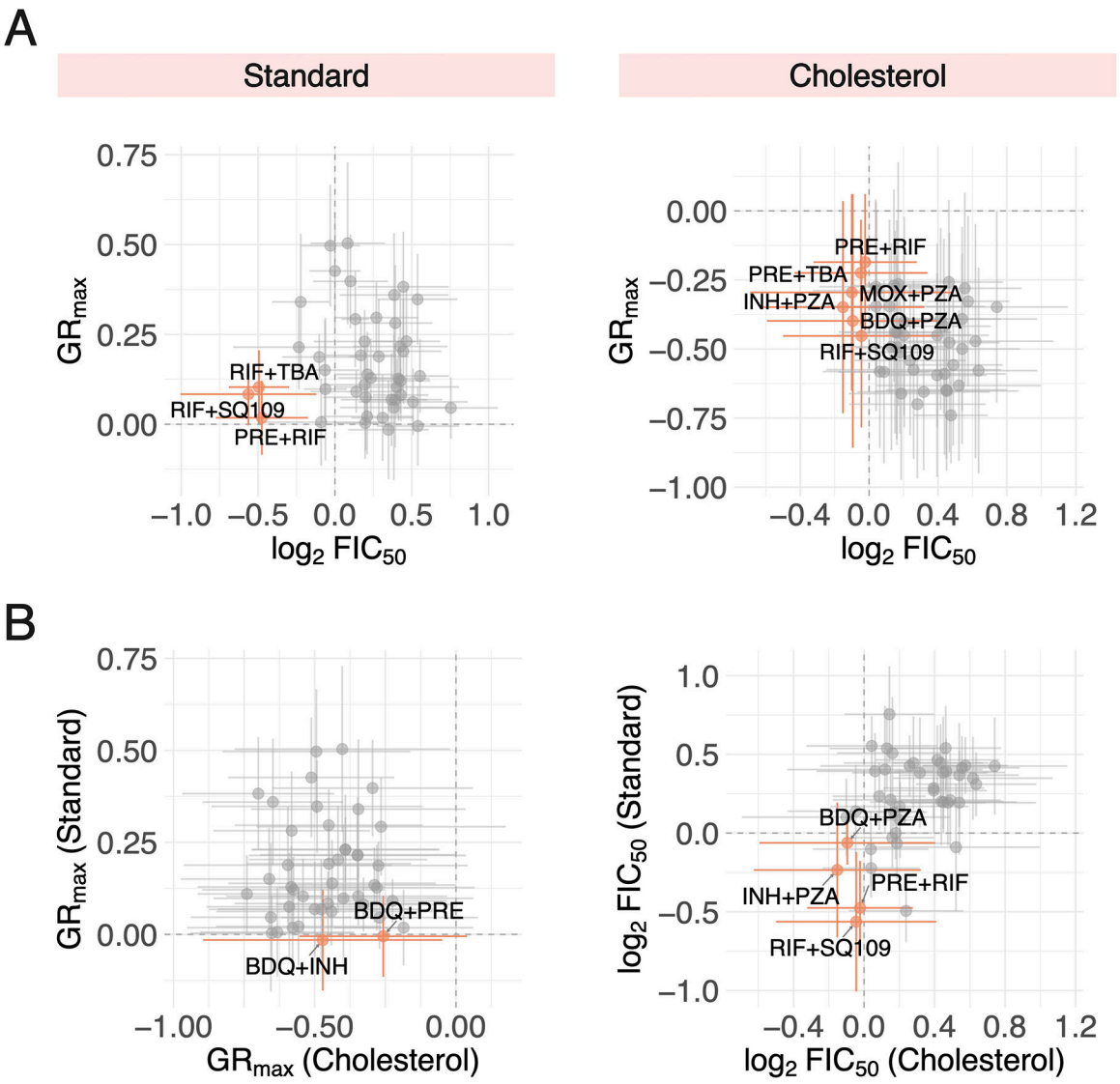

Figure 4. Comparison of drug pairs combination treatment responses across different *in vitro* conditions and dose response metrics.

(A) Potent (low GR_{max} value) and synergistic (low log_2FIC_{50} value) drug pairs identified in *in vitro* conditions. (Left) The three drug pairs with the lowest mean GR_{max} and log_2FIC_{50} values are represented by orange points. All other drug pairs are represented by grey points. Vertical and horizontal bars denote standard deviation of GR_{max} and log_2FIC_{50} values, respectively. (Right) Drug pairs that are both cytotoxic and synergistic, indicated by negative GR_{max} and log_2FIC_{50} values, respectively, are represented by orange points. (B) (Left) Drug pairs that are cytotoxic (negative GR_{max} value) in both standard and cholesterol conditions are represented by orange points. Vertical and horizontal bars denote the standard deviation of GR_{max} values and standard and cholesterol, respectively. (Right) Drug pairs that are synergistic (negative log_2FIC_{50} value) in both standard and cholesterol conditions are represented by orange points.